



Replacement and desmoplastic histopathological growth patterns in cutaneous melanoma liver metastases: frequency, characteristics, and robust prognostic value

Raymond Barnhill^{1,2,3*} , Pieter-Jan van Dam^{4,5†}, Peter Vermeulen^{4†}, Gabriel Champenois⁶, André Nicolas⁶, Robert V Rawson^{7,8,9}, James S Wilmott^{7,8,9}, John F Thompson^{7,9,10}, Georgina V Long^{7,9,11}, Nathalie Cassoux^{3,12}, Sergio Roman-Roman², Klaus J Busam¹³, Richard A Scolyer^{7,8,9}, Alexander J Lazar^{14,15,16,17}  and Claire Lugassy² 

¹Department of Pathology, Institut Curie, Paris, France

²Department of Translational Research, Institut Curie, Paris, France

³Faculty of Medicine, University of Paris René Descartes, Paris, France

⁴Faculty of Medicine and Health Sciences, University of Antwerp – MIPRO Center for Oncological Research (CORE) – TCRU, GZA Sint-Augustinus, Antwerpen, Belgium

⁵HistoGeneX, Wilrijk, Belgium

⁶Experimental Pathology, Department of Pathology, Institut Curie, Paris, France

⁷Melanoma Institute Australia, The University of Sydney, Sydney, Australia

⁸Department of Tissue Pathology and Diagnostic Oncology, Royal Prince Alfred Hospital and NSW Health Pathology, Sydney, Australia

⁹Sydney Medical School, The University of Sydney, Sydney, Australia

¹⁰Department of Surgery, Royal Prince Alfred Hospital and NSW Health Pathology, Sydney, Australia

¹¹Department of Medical Oncology, Northern Sydney Cancer Centre, Royal North Shore Hospital, Sydney, Australia

¹²Department of Ophthalmology, Institut Curie, Paris, France

¹³Department of Pathology, Memorial Sloan Kettering Cancer Center, New York, NY, USA

¹⁴Department of Pathology, The University of Texas MD Anderson Cancer Center, Houston, TX, USA

¹⁵Department of Genomic Medicine, The University of Texas MD Anderson Cancer Center, Houston, TX, USA

¹⁶Department of Dermatology, The University of Texas MD Anderson Cancer Center, Houston, TX, USA

¹⁷Department of Translational Molecular Pathology, The University of Texas MD Anderson Cancer Center, Houston, TX, USA

*Correspondence: Raymond Barnhill, Department of Translational Research, Institut Curie, 26 rue d'Ulm, 75248 Paris cedex 05, France.
E-mail: raymond.barnhill@curie.fr

†These authors contributed equally to this work.

Abstract

Among visceral metastatic sites, cutaneous melanoma (CM) metastasises initially to the liver in ~14–20% of cases. Liver metastases in CM patients are associated with both poor prognosis and poor response to immunotherapy. Histopathological growth patterns (HGPs) of liver metastases of the replacement and desmoplastic type, particularly from colorectal cancer and uveal melanoma (UM), may impart valuable biological and prognostic information. Here, we have studied HGP in 43 CM liver metastases resected from 42 CM patients along with other prognostic factors from three institutions. The HGPs (replacement, desmoplastic, pushing) were scored at the metastasis–liver interface with two algorithms: (1) 100% desmoplastic growth pattern (dHGP) and any (≥1%) replacement pattern (any-rHGP) and (2) >50% dHGP, >50% rHGP or mixed (<50% dHGP and/or rHGP, pushing HGP). For 1 patient with 2 metastases, an average was taken to obtain 1 final HGP yielding 42 observations from 42 patients. 22 cases (52%) had 100% dHGP whereas 20 (48%) had any replacement. Cases with rHGP demonstrated vascular co-option/angiotropism. With the development of liver metastasis, only rHGP (both algorithms), male gender and positive resection margins predicted diminished overall survival ($p = 0.00099$ and $p = 0.0015$; $p = 0.034$ and $p = 0.024$ respectively). On multivariate analysis, only HGP remained significant. 7 of 42 (17%) patients were alive with disease and 21 (50%) died with follow-up after liver metastases ranging from 1.8 to 42.2 months (mean: 20.4 months, median: 19.0 months). 14 (33%) patients with previously-treated metastatic disease had no evidence of disease at last follow up. In conclusion, we report for the first time replacement and desmoplastic HGPs in CM liver metastases and their prognostic value, as in UM and other solid cancers. Of particular importance, any rHGP significantly predicted diminished overall survival while 100% dHGP correlated with increased survival. These results contribute to a better understanding of the biology of CM liver metastases and potentially may be utilised in managing patients with these metastases.

Keywords: cutaneous melanoma; metastasis; liver; histopathological growth patterns; replacement; desmoplastic; vascular co-option; angiotropism; pericytic mimicry; extravascular migratory metastasis

Received 19 December 2019; Revised 10 February 2020; Accepted 14 February 2020

Conflict of interest statement: RAS has received fees for professional services from Merck Sharp & Dohme, GlaxoSmithKline Australia, Bristol-Myers Squibb, Dermepedia, Novartis Pharmaceuticals Australia Pty Ltd, Myriad, NeraCare and Amgen. The other authors declare no conflicts of interest.

Introduction

Mortality in patients with cutaneous melanoma (CM) is directly related to the development of visceral metastases. Among the principal visceral metastatic sites of the brain, liver and lungs, CM metastasises initially to the liver in some 14–20% of cases [1–5]. Consequently, hepatic metastases from CM may be an important determinant of the clinical outcome and effective management remains a therapeutic challenge [2].

Obtaining adequate material for research remains a substantial stumbling block for comprehensive investigation of hepatic metastases originating from melanoma and other solid tumours [6]. In particular, satisfactory and sufficiently large liver samples of metastatic CM resected from living patients are rarely obtained in the modern era. Conversely, the liver is a frequent site of metastasis for tumours originating from the gastrointestinal tract, pancreas, breast, and lung [7–11]. Liver metastases from colorectal and breast cancers have been extensively studied and show distinctive ‘histopathological growth patterns’ (HGP) [7–11]. In brief, these HGPs constitute: ‘replacement’, ‘desmoplastic’, ‘pushing’ and two rare variants – the ‘sinusoidal’ and ‘portal’ HGPs. The HGPs are represented by a distinctive interface between cancer cells and the adjacent normal liver parenchyma that can be recognised by conventional microscopy. In brief, the replacement HGP is defined by tumour cells from the metastasis infiltrating and forming plates in continuity with the surrounding hepatic parenchymal plates and perpendicular to the tumour–liver interface [6]; the desmoplastic HGP by a distinct separation of the metastasis by a peripheral annulus (band) of desmoplastic fibrous tissue [6]; the pushing pattern by compression and pushing away of hepatic plates by the metastasis without tumour cells invading the liver plates [6]; the sinusoidal pattern by the presence of tumour cells in sinusoidal blood vessels or perisinusoidal spaces in between the liver plates; and the portal pattern by the metastasis being restricted to the portal tracts [8]. The distinctive topography of cancer

cells in each HGP predicts HGP-specific interactions with parenchymal cells (hepatocytes and cholangiocytes) and non-parenchymal cells (sinusoidal endothelial cells, pericytes/stellate cells and immune cells) of the liver. Importantly, the HGPs of liver metastases from these tumours have prognostic significance [7–11].

We have recently reported for the first time the frequency of the replacement and desmoplastic histopathological patterns (HGPs) in uveal melanoma liver metastases (UMLM) resected from living patients and their important prognostic value for UM patients, similar to those described in other solid cancers [6].

For over a century, it has been reasoned that lymphatic and haematogenous dissemination may account for virtually all metastases. However, the latter routes of tumour spread must take into consideration the temporal variation and latency in the appearance of metastases. The latter could potentially be explained by (1) the formation of dormant metastases after intravascular spread [12] and/or (2) extravascular migratory metastasis (EVMM), i.e. a step-by-step migration from the primary tumour to the site of metastasis [13]. In both CM and UM, we have described the association of tumour cells with the abluminal surfaces of vascular channels, which is termed angiotropism [13]. Importantly, we have shown in a recent study that the terms ‘co-option’ and ‘angiotropism’ appear to connote a similar histopathological image, and probably a close and complementary biological phenomenon [14]. Angiotropic tumour cells can spread along the abluminal surfaces of vessels without entering the vascular channels (intravasation), therefore making use of the blood vascular network as a track [13]. As mentioned above, this tumour cell migration has been termed EVMM and is believed to represent an embryogenesis-derived programme of tumour spread independent of intravasation and haematogenous dissemination [13]. Because of the biological and prognostic importance of angiotropism in melanoma in general [6,12–17], and also because of the adverse prognostic effect of

the replacement HGP (co-option/ angiotropism) recently described in UM [6] and in other solid tumours [7–11], we have undertaken new investigations of liver metastases from CM.

Herein we have examined 43 liver metastases resected from 42 patients with CM for the presence of specific HGPs and analysed their prognostic significance.

Materials and methods

This study was approved by the institutional ethics committees of the Melanoma Institute of Australia; Memorial Sloan Kettering Cancer Center; and The University of Texas MD Anderson Cancer Center. Written informed consent for the use of tissue specimens and data for research was signed by each patient. The study complied with the principles of the Declaration of Helsinki.

Patient information

We have examined the HGPs in 43 CM liver metastases resected from 42 patients along with other prognostic factors from three institutions.

Forty-three hepatic metastases from 42 patients with UM were retrieved from the anatomic pathology archives of three institutions: 16 cases from the Melanoma Institute of Australia; 5 cases from Memorial Sloan Kettering Cancer Center and 21 from The University of Texas MD Anderson Cancer Center from the period 2001 to 2018. Clinical, histopathological, genetic, and long-term follow-up information for these patients has been collected retrospectively as previously described [6,19]. The following patient characteristics were analysed and most variables are displayed in Table 1: age (years); gender; anatomic site of the primary tumour (unknown; head and neck; trunk; extremities, non-acral; acral); Breslow thickness of the primary melanoma (mm); presence or absence of ulceration of the primary melanoma; mutational analysis of the primary melanoma (see below); adjuvant therapy of the primary melanoma (none; anti-BRAF/MEK; immunotherapy; other such as radiotherapy); sentinel lymph node biopsy status (not done, positive, negative); disease-free interval (date of primary tumour diagnosis to metastasis); Resection status of metastasis: R0 – resection complete, R1 – microscopically incomplete, R2 – macroscopically incomplete); initial therapy of liver metastases (surgery alone, surgery plus systemic therapy, any systemic therapy); and overall survival.

Table 1. Patient characteristics

	n = 42 (%)
Patient characteristics	
Gender (female)	20 (48%)
Age at diagnosis (years) (MD = 7)	
Mean (SD)	51.5 (15.4)
Median (range)	52 (19–78)
Site of primary melanoma (no MD)	
Unknown	11 (26%)
Head and neck	9 (21%)
Trunk	13 (31%)
Extremities, non-acral	8 (19%)
Acral	1 (2%)
Primary tumour characteristics	
Breslow thickness (BT) (mm) (MD = 16)	
Mean (SD)	2.9 (1.8)
Median (range)	2.5 (0.9–8.6)
Ulceration (MD = 18)	
Absent	14 (58%)
Present	10 (42%)
Sentinel lymph node biopsy (no MD)	
No	27 (64%)
Yes, positive	5 (33%)
Yes, negative	10 (67%)
Mutation analysis (n = 10) (MD = 21)	
Not done	21 (68%)
<i>BRAF</i>	6 (19%)
<i>NRAS</i>	0 (0%)
<i>KIT</i>	1 (3%)
Triple negative	3 (10%)
Adjuvant treatment (no MD)	
None	24 (57%)
Anti-BRAF/MEK	1 (2%)
Immunotherapy	12 (29%)
Other, X-irradiation	8 (19%)
Disease-free interval (time to metastasis; MD = 7) (months)	
Mean (SD)	56.7 (72.9)
Median (range)	32 (0–340)
First treatment of mets (MD = 3)	
Surgery	24 (62%)
Surgery and systemic	15 (38%)
Resection margins when surgery (MD = 5)	
R0	32 (87%)
R1	3 (8%)
R2	2 (5%)
Overall survival from diagnosis of mets (months) (no MD)	
Mean (SD)	41 (47.4)
Median (range)	26 (2–204)
First treatment: surgery alone (months)	n = 24
Mean (SD)	43 (57.5)
Median (range)	18 (2–204)
Surgery + systemic treatment (months)	n = 13
Mean (SD)	44 (33.8)
Median (range)	33 (6–125)
Any systemic treatment (months)	n = 2
Mean (SD)	17 (3.1)
Median (range)	17 (15–19)

MD, missing data.

Histopathology

Formalin-fixed, paraffin-embedded (FFPE) 5- μ m sections were prepared for each liver metastasis for microscopic examination. Whole glass slides were digitised with a Phillips pathology slide scanner (Phillips Healthcare, Amsterdam, the Netherlands). Criteria for the selection of metastases were as follows: if more than one metastasis was present, criteria for selection included metastases having a 360° circumference surrounded by viable intact liver parenchyma, or those with the highest percentage of the peripheral circumference (of the metastasis) surrounded by liver parenchyma, and absence of significant necrosis, scarring, or disruption of either the metastasis or the liver. Histopathological characteristics recorded based on the examination of representative haematoxylin and eosin-stained sections or digital images for each case included: the HGP of the liver metastases; diameter of each metastasis (nodule in mm), and angiotropism of melanoma cells. If more than one tissue section per case was available for each metastasis, the mean diameter was determined. The HGP was scored according to consensus guidelines as described by van Dam *et al* [8]. The liver metastasis HGP assessment consisted of the percentage of the circumference involved by

desmoplastic, replacement, or pushing HGP. The HGPs (replacement, desmoplastic, pushing) were scored at the metastasis–liver interface in a continuous fashion with two algorithms: (1) 100% desmoplastic growth pattern (dHGP) and any-replacement pattern (any-rHGP), including $\geq 1\%$ replacement pattern or any non-replacement mixed pushing-desmoplastic pattern [11]; and (2) $>50\%$ dHGP, $>50\%$ rHGP, or mixed ($<50\%$ dHGP and/or $<50\%$ rHGP, and potentially any pushing HGP) [6]. For one patient with two metastases, an average was taken to obtain 1 final HGP per patient yielding 42 observations from 42 patients. Data from both algorithms were analysed. Angiotropism was defined as previously described [6,13,19]: melanoma cells arrayed along the abluminal vascular surfaces of sinusoidal vessels (in the space of Disse) and/or along portal venules in the portal tracts. In particular, this included (1) clearly recognisable (unequivocal) melanoma cells disposed circumferentially, radially or longitudinally along the abluminal (external) surfaces of the endothelium of microvascular channels either in single-layered or multi-layered arrangements; (2) the latter occurring in at least one or more foci; and (3) there was no evidence of intravascular melanoma cells.

The images were reviewed independently by two experienced senior pathologists (PV and RB) without specific knowledge of the case or clinical outcome.

Table 2. Characteristics of liver metastases

Histopathological growth patterns	<i>n</i> = 42 (%)
Any replacement versus 100% desmoplastic pattern	
Any replacement ($\geq 1\%$ replacement [<i>n</i> = 19], any % pushing)	20 (48%)
Desmoplastic (100%)	22 (52%)
Predominant pattern ($>50\%$)	
Replacement ($>50\%$)	14 (73%)
Mixed ($<50\%$ replacement, $<50\%$ desmoplastic, any % pushing)	5 (12%)
Desmoplastic ($>50\%$)	23 (55%)
Metastasis diameter	<i>n</i> = 42
Metastasis diameter (mm) (<i>n</i> = 42)	
Mean (SD)	13.7 (5.6)
Median (range)	13 (4–26)
Any replacement diameter (mm) (<i>n</i> = 20)	
Mean (SD)	13.7 (6.6)
Median (range)	12.4 (5–25)
Desmoplastic diameter (mm) (<i>n</i> = 22)	
Mean (SD)	13.6 (4.5)
Median (range)	13 (4–26)
Mutation analysis	
Mutation analysis (<i>n</i> = 17) (MD = 25)	
Not done	25 (60%)
<i>BRAF</i>	9 (21%)
<i>NRAS</i>	2 (5%)
<i>KIT</i>	0 (0%)
Triple negative	6 (14%)

MD, missing data.

Immunohistochemistry

FFPE sections from one metastasis showing a replacement HGP and one with desmoplastic HGP were examined by immunohistochemistry with melan-A (Agilent [Dako], clone A103, dilution 1/50). A Vector Red chromogen was utilised. Peroxidase activity was developed using 3-amino-9-ethylcarbazole and H_2O_2 , and the slides were counterstained with haematoxylin.

Genetic analysis

Among the 42 patients, 10 primary tumours and 17 liver metastases underwent mutation analysis and the results recorded (not done, *BRAF*, *NRAS*, *KIT*, other) (Tables 1 and 2).

Statistical analyses

Data were analysed using R statistical software (<https://cran.r-project.org>). The relationships between HGP and other categorical variables were evaluated by

the Fisher's exact test. The survival analyses included overall survival (OS) and disease-free (metastasis-free) survival (DFS). Patients were censored when alive at last follow-up or when lost to follow-up. Overall Survival was defined as the difference between time of diagnosis of the metastasis (OS metastasis) and time of death or last follow-up, or the difference between time of diagnosis of the primary CM (OS primary) and time of death or last follow-up. Differences in survival were calculated using log-rank test. Univariate and multivariate hazard ratios were calculated using Cox proportional hazards model. All statistical tests were considered significant with P value <0.05 . Since we did not know if there was any effect among the HGP, and the other clinical variables, we opted to keep all the variables in the multivariate analysis in order to adjust for confounding and suppression of variables in our data set [20]. Removing the variables that were not significant in univariate analysis could lead to the exclusion of possible significant variables due to suppression.

Results

Patient and primary melanoma characteristics

The patient clinical information and primary tumour characteristics are summarised in Table 1.

The study population constituted 20 (48%) women and 22 men. About 31 patients had widely distributed primary tumours, whereas 11 (26%) had no established primary site (unknown primary). Breslow thickness mean was 2.9 mm and median 2.5 mm (range: 0.9–8.6 mm). Ten (42%) melanomas were ulcerated. Among 15 patients (36%) undergoing sentinel lymph node biopsy, only 5 (33%) were reported as positive for metastatic melanoma. Mutation analysis was performed for 10 patients. Six patients had *BRAF V600E* mutations; a *KIT* mutation; and three were not mutated in *BRAF*, *NRAS* or *KIT*.

Seven of 42 (17%) patients were alive with disease and 21 (50%) patients died with a follow-up ranging from 2 to 204 months (mean: 41 months, median: 26 months). Fourteen (33%) patients with previously treated metastatic disease had no evidence of disease at last follow up. The mean and median disease-free survival (DFS) intervals were 57 and 32 months, respectively, with a range of 0–340 months. Overall survival after the following therapies for metastatic disease was: surgery alone – mean 43 months, median 18 (range 2–204); surgery plus systemic therapy –

mean 41 months, median 32 (range 6–126; $p = 0.93$ log-rank test).

Categorisation of metastases by HGP

Analysis of HGP and diameter of metastases is summarised in Table 2. Initial independent blinded review of the HGP in the 43 metastases by the two pathologists revealed good to excellent general agreement for 35 cases, whereas 7 cases (17% of the 42 cases) resulted in some initial discordance. The pathologists reached concordance by review and discussion by webinar and final consensus reached during these discussions. (1) 20 (48%) cases had an *any* replacement pattern and 22 (52%) metastases a pure (100%) desmoplastic pattern. Among the *any* replacement category, three cases showed neither 100% desmoplastic pattern nor *any* replacement pattern. These cases had combined desmoplastic-pushing patterns as follows: 95% dHGP: 5% pHGP, 80% dHGP: 20% pHGP and 20% dHGP: 80% pHGP. Among these 20 cases, 13 (31%) metastases had a pure (100%) rHGP. (2) 14 (33%) metastases had a predominant ($>50\%$) rHGP and $<50\%$ dHGP, 23 (55%) metastases a predominant ($>50\%$) dHGP and $<50\%$ rHGP, and 5 (12%) cases characterised by $<50\%$ rHGP and $<50\%$ dHGP, and a pHGP ranging from 5 to 80%. In 13 of 42 cases, at least 1 level section was obtained, and the predominant HGP did not change in any case. Metastasis diameters were analysed and compared by predominant HGP (Table 2). For the entire cohort, metastases ranged in size (diameter) from 4 to 26 mm with mean of 13.7 mm and median of 13 mm, and there was no significant difference in size between the replacement and desmoplastic metastases ($p = 0.75$ using Mann–Whitney U test).

Almost one half (48%) of the metastases were classified as having *any* replacement HGP (≥ 1 to 100%). These metastases were characterised by non-destructive infiltration of the surrounding liver hepatic plates, progressive replacement of hepatocytes by melanoma cells (Figure 1) and preservation of the liver architecture (Figure 1A–D). Individual melanoma cells were aligned along the external (abluminal) surfaces of the sinusoidal vascular channels. A striking feature associated with many of these metastases was the radial extension of individual melanoma cells considerable distances (up to 1 mm) away from the central metastatic focus into the surrounding liver parenchyma (Figure 1B–D). The melanoma cells were apparently localised to the space of Disse. Within many of these metastases, one could observe a complete replacement of hepatocytes by melanoma cells in the hepatic plates.

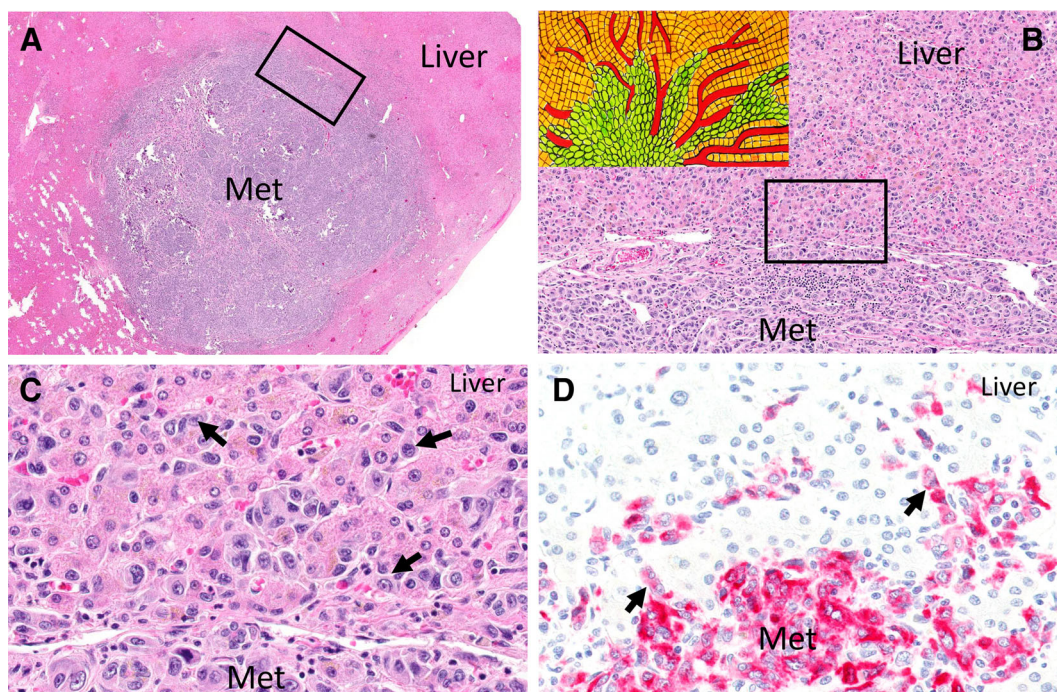


Figure 1. Replacement histopathological growth pattern (HGP). (A) Scanning magnification shows a fairly discrete metastasis (Met) with surrounding liver parenchyma (Liver). The box indicates the poorly defined metastasis–liver interface. (B) The interface (box) between the metastasis proper (most inferior portion of field) and surrounding liver parenchyma is poorly defined. Melanoma cells are dispersed throughout this interface and the surrounding hepatocytic plates as single cells, files of cells, and in small clusters beyond the main portion of the metastasis. These cells replace hepatocytes in the hepatic plates without altering their architecture or the architecture of the sinusoidal vasculature. Inset (upper left) illustrates the replacement HGP. The hepatic parenchyma (yellow) is infiltrated and replaced by melanoma cells (green). The melanoma cells are disposed along the abluminal surfaces of the sinusoidal vessels (red). (C) Melanoma cells (arrows) extending into the surrounding hepatic plates (Liver) some distance from the metastasis (Met) along the sinusoidal vessels. (D) Melan-A immunostain with red chromogen highlights melanoma cells (arrows) extending into the surrounding liver parenchyma (Liver) along the external surfaces of sinusoidal vascular channels from the metastatic nodule (Met).

There was no evidence of melanoma cells within the lumina of the sinusoidal vessels. Within the portal triads of some of these metastases, melanoma cells were disposed along the abluminal surfaces of portal venous vessels (angiotropism). In such metastases, variable perivascular lymphocytic infiltrates were often seen.

Twenty two (52%) of the metastases showed a 100% desmoplastic HGP. These tumours were well-circumscribed with complete separation of the metastasis from the surrounding liver parenchyma by an annulus of dense desmoplastic collagen (Figure 2A–E). Within the metastatic nodule, there was complete obliteration of the liver architecture. In general, these metastases showed prominent peri-tumoural infiltrates of lymphocytes localised to the desmoplastic–liver parenchymal interface (Figure 2C,D). Usually, tumour-infiltrating lymphocytes were sparse or absent.

Five metastases were classified as mixed because of the composition of the pushing-HGP, associated with <50%

desmoplastic and/or <50% replacement components [8]. The pHGP in each instance comprised 5, 32 (mean), 40, 55% (mean), and 80% of the circumference of the metastasis (Figure 3). Two additional metastases had a 5 and 20% pHGP, respectively, but also a predominant 95 and 80% dHGP, respectively.

Mutation analysis

Mutation analysis was performed for the liver metastases from 17 patients. Nine patients had *BRAF* V600E mutations; two *NRAS* mutations; and six were not mutated in *BRAF*, *NRAS* or *KIT* (Table 2). The *BRAF* and *NRAS* mutations showed no association with HGP.

Immunohistochemistry

Immunohistochemical evaluation of one replacement and one desmoplastic metastasis with melan-A showed

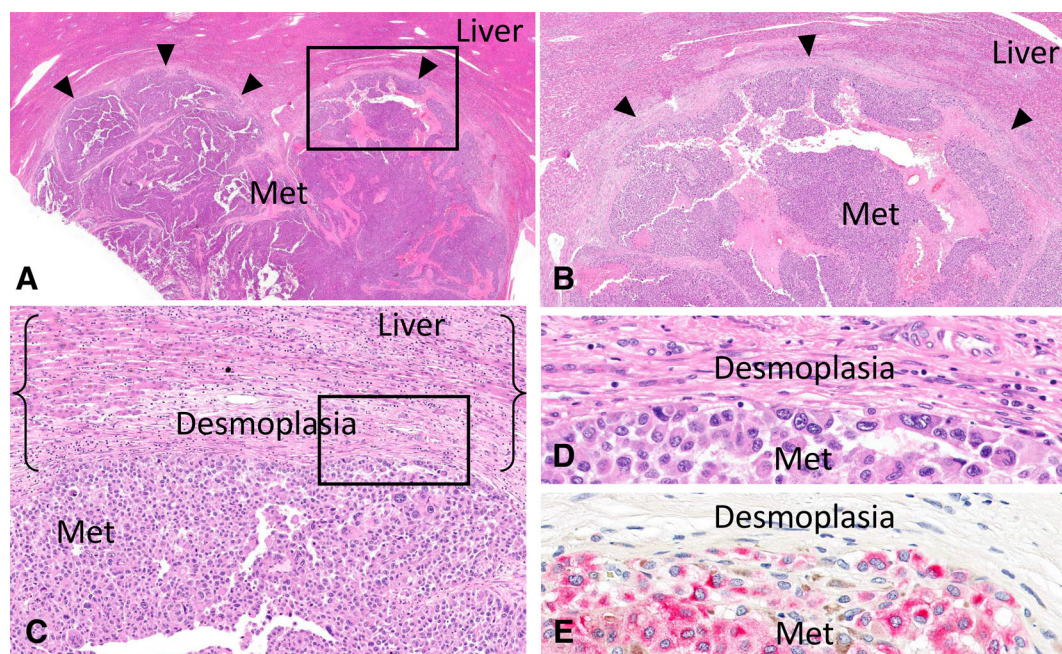


Figure 2. Desmoplastic histopathological growth pattern (HGP). (A) Scanning magnification depicts a metastasis (Met, inferior part of the field) with abrupt desmoplastic interface (arrowheads) separating the tumour from the surrounding liver parenchyma (box) (Liver, superior part of the field). The liver architecture is completely obliterated by the tumour mass. (B) An annulus of dense desmoplastic collagen (arrowheads) constitutes this interface between the metastasis (Met, inferior) and the liver parenchyma (Liver) observed in the superior half of this field. (C) High magnification of (B) showing the interface of the desmoplastic annulus (box, Desmoplasia) separating the liver parenchyma (Liver) completely from the metastasis (Met). Brackets indicate the peri-tumoural zone containing lymphocytic infiltrates. This zone includes the outer part of the desmoplastic annulus and an adjoining rim of liver parenchyma (Liver). (D) Higher magnification of C, showing metastasis (Met)–liver interface with desmoplastic annulus (Desmoplasia). (E) Melan-A immunostain (red chromogen) highlights melanoma cells (Met) separated from liver parenchyma by the band of desmoplasia.

striking localisation of melanoma cells within hepatic plates along the external surfaces of the sinusoidal vascular channels (Figure 1D). This vascular-cooption/angiotropism was best visualised at the metastasis–liver parenchymal interface and in the immediately surrounding peri-tumoural liver parenchyma. There was no clear-cut evidence of melanoma deposits within the sinusoidal vascular lumina. In the dHGP, melan-A highlighted melanoma cells encased within a sharply delimited nodule by a dense band of desmoplastic collagen (Figure 2E).

Overall survival after the development of hepatic metastatic disease

Examination of how HGP might potentially influence survival after the development of liver metastases from CM was the primary objective of this study. Univariate analysis with the log-rank test showed that HGP when analysed by the two algorithms had a striking effect on overall survival (OS metastasis) ($p = 0.0099$ (100% dHGP versus any rHGP algorithm) (Figure 4); and $p = 0.0015$ (>50% algorithm) (Figure 5). In

particular, the replacement pattern had a clearly adverse effect on survival as compared to the protective effect of the desmoplastic pattern, irrespective of the percentage replacement-HGP present, i.e. >1% versus >50%. Five cases with mixed-HGP (including four cases with any rHGP and one with 80% pHGP) were associated with poor survival. It is important to emphasise that pure dHGP conferred unique survival advantage apart from other HGP variants [10].

The only other variables having significant predictive value for OS on univariate analysis were gender ($p = 0.034$) and R0 complete resection status ($p = 0.024$). None of the other variables including primary tumour location, Breslow thickness, ulceration of the primary tumour, treatment of the primary tumour, mutations, metastasis size, and the various treatments for metastatic disease had any significant effect on survival.

On multivariate analysis with the Cox proportional hazards model, HGP continued to show a significant effect with a hazard ratio (HR) of 3.79 (1.33–10.83) with $p = 0.01$ (Table 3). While none of the other

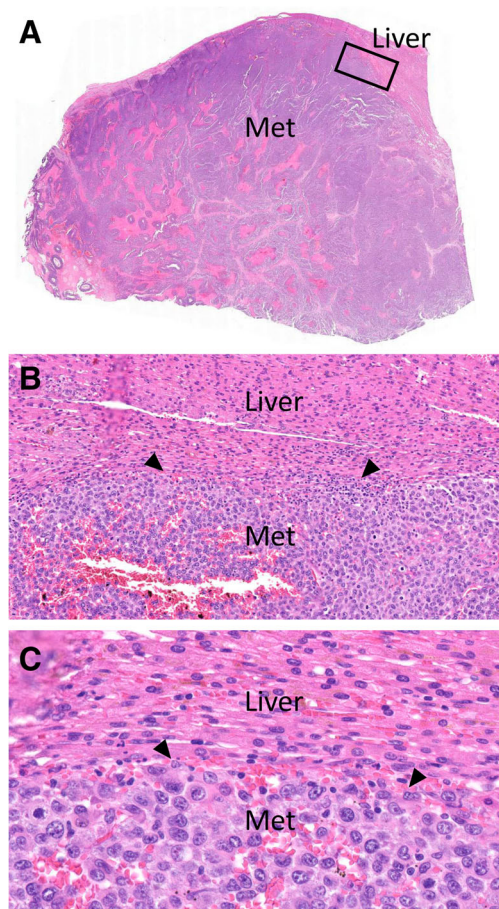


Figure 3. Pushing histopathological growth pattern (HGP). (A) Scanning magnification shows a large discrete metastasis. The metastasis–liver interface is indicated by the box. (B) The metastatic nodule (Met, inferior half of field) compresses the overlying liver parenchyma (Liver, superior half of field) with horizontal disposition of hepatic plates. The metastasis–liver interface (arrowheads) is abrupt and characterised by the absence of desmoplasia and no infiltration of the overlying hepatic parenchyma. (C) Higher magnification of (B) melanoma cells (Met) do not invade the liver cell plates (Liver, superior) and desmoplasia is absent at the interface (arrowheads) between the metastasis and the liver parenchyma. Note the horizontal orientation of hepatocytes; this is not desmoplasia.

prognostic factors were significant, gender showed a trend towards significance ($p = 0.06$).

Overall survival analysed from the date of diagnosis of the primary CM

When OS was analysed from the date of diagnosis of the primary CM using the log-rank test, HGP was not statistically significant. On univariate analysis, other conventional prognostic factors such as patient age, Breslow thickness, ulceration, *etc.* did not show any

predictive value. Only ‘time to metastasis’ ($p = 0.02$) and liver metastasis resection margins ($p = 0.02$) were significantly different. However, on multivariate analysis, none of the variables remained significant.

Disease-free (metastasis-free) survival analysis

On univariate analysis, none of the variables were significant, with only sentinel node biopsy status trending towards significance ($p = 0.06$). Examination of HGP in this context of DFS, as expected, had no predictive value. On multivariate analysis, none of the variables remained significant.

Discussion

In the current work, we have described for the first time HGP in liver metastases originating from CM (CMLM). In accordance with international consensus guidelines for HGP [8], and previous studies of liver metastases from colorectal carcinoma (CRC), breast carcinoma, and UM [6,11], we have utilised the standardised terms ‘replacement, desmoplastic, and pushing’ to depict HGP. Independent review of cases by two pathologists without any knowledge of patient outcome confirmed good concordance, as in previous studies [6,8].

The current study was conducted in a similar fashion to our previous investigation of UMLM, except that two diagnostic algorithms were used in this study. The rationale for implementing a second algorithm of 100% desmoplastic and *any* replacement ($\geq 1\%$) HGPs was based on the strikingly adverse effect of *any* replacement-HGP *versus* the favourable prognostic effect of 100% desmoplastic-HGP on overall survival in CRC [11]. In addition, metastatic disease usually progresses from a more favourable status (desmoplastic pattern) to one more adverse (replacement pattern), accompanied by a deteriorating clinical course, and not the converse [10]. Consequently, any element of replacement-HGP supervening in an existing desmoplastic metastasis is believed to override adversely the protective effect of the desmoplastic-HGP [11].

The other algorithm, as in our previous study of UM [6], involved classification of metastases as the predominant pattern, e.g. $>50\%$ replacement HGP, $>50\%$ desmoplastic pattern, or as a mixed pattern with $<50\%$ replacement, $<50\%$ desmoplastic, and any pushing HGP. As described, our results were very similar morphologically to those associated with CRC, breast carcinoma, and more recently with UM [6,8].

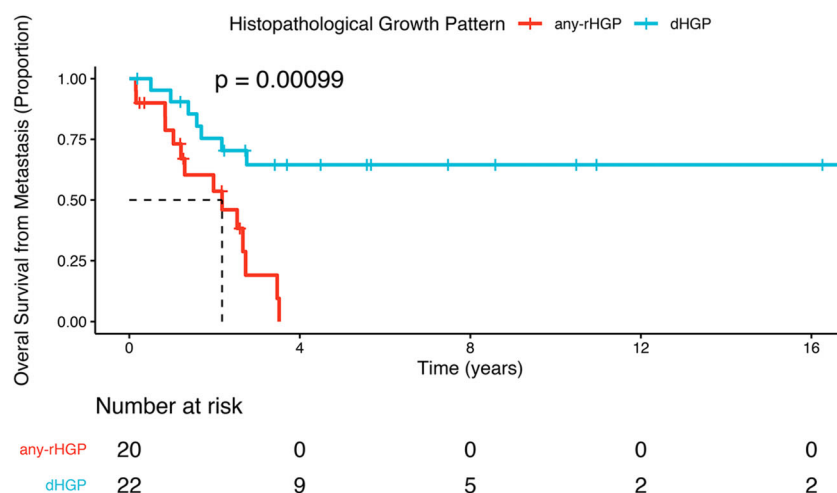


Figure 4. The effects of any replacement and 100% desmoplastic HGPs of CM liver metastases on overall survival analysed by the log-rank test with Kaplan–Meier plots. Overall survival is from the time of diagnosis of liver metastases to death or to date of last follow-up.

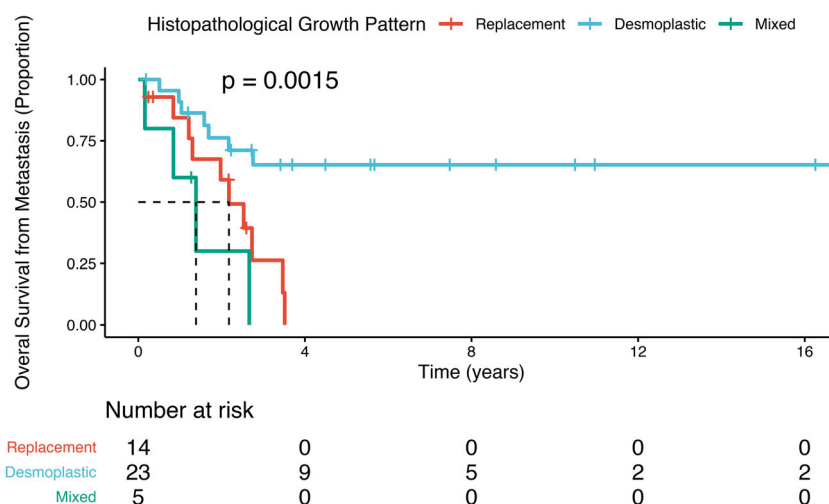


Figure 5. The effects of >50% replacement, >50% desmoplastic, and mixed HGPs of CM liver metastases on overall survival analysed by the log-rank test with Kaplan–Meier plots. Overall survival is from the time of diagnosis of liver metastases to death or to date of last follow-up.

Table 3. Cox proportional hazards analysis for factors predictive of death from time of metastasis

Variables		Univariate		Multivariate	
		HR (95% CI)	P value	HR (95% CI)	P value
Histopathological growth pattern	Any replacement	3.92 (1.50–10.22)	0.005	3.79 (1.33–10.83)	0.01
Tumour nodule	Continuous	1.02 (0.92–1.12)	0.7	1.06 (0.96–1.18)	0.24
Gender	Male	2.98 (1.15–7.73)	0.02	2.71 (0.97–7.55)	0.06
Resection margins	R1/R2	3.51 (1.10–11.15)	0.03	2.81 (0.61–13.00)	0.19
Treatment of liver metastasis	Surgery	1.17 (0.47–2.90)	0.7	1.39 (0.48–4.01)	0.55

Bold font indicates statistically significant values.

The histomorphological features of CMLM are indistinguishable from UMLM. Metastases with the replacement HGP showed a characteristic poorly

defined interface with the liver parenchyma because of progressive infiltration and replacement of the hepatic plates by melanoma cells. Thus the architecture of both

the liver parenchyma and the sinusoidal vasculature were preserved. Melanoma cells were aligned along the abluminal surfaces of the sinusoidal vessels in the Space of Disse. In a similar fashion, CMLM of the desmoplastic type, as UMLM, exhibited a sharply delimited interface: a dense (desmoplastic) band of fibrous tissue isolating the metastasis completely from the surrounding liver parenchyma. The architecture of the liver and corresponding vasculature are completely altered. Seven (17%) metastases showed some element of the pushing HGP in combination with the desmoplastic HGP in all cases and the replacement HGP in four cases. Pushing components were characterised by expansile nodular compression of the surrounding liver parenchyma with a well-defined tumour–liver interface and the absence of both desmoplasia and infiltration of the liver parenchyma by tumour cells. In general, CMLMs were less pigmented than UMLMs. It is of interest that a greater frequency of both pure and predominant desmoplastic HGPs appear associated with CMLR *versus* that observed in UMLM [6]. However, the study of larger numbers of cases is needed to establish with greater certainty the prevalence of these growth patterns in both forms of melanoma. Nonetheless, the observation of comparable morphological findings across multiple tumour types and those with different developmental origins provides additional important support for the biological basis and the generalisability of these HGPs in cancer metastases.

An observation of fundamental importance from our study that parallels that recently established in UM is the robust prognostic value of the replacement and desmoplastic HGPs. In a similar fashion to UM, CRC, and breast carcinoma, [6,8,11], the presence of *any replacement* pattern significantly predicted diminished overall survival while the desmoplastic pattern correlated with increased survival. The striking effect of *pure* dHGP *versus* *any* replacement (or the rare pushing) HGP, has confirmed this singular effect of 100% dHGP demonstrated recently in CRC [11]. These findings potentially provide for the first time an important tissue biomarker for prognosis after the development of CMLM. In our study, once metastases had developed, OS diminished significantly ($p = 0.00099$) in patients with *any replacement HGP*. Although the examination of greater numbers of cases is needed, a point of particular importance is that metastases with <50% (perhaps even <10–20%) of the metastasis interface exhibiting the replacement HGP may have conspicuous predictive value for an adverse outcome. In addition, this predictive effect continues to be significant on multivariate analysis (HR = 3.79, $p = 0.01$) (Table 3). Since the replacement HGP, also termed

infiltrative or non-angiogenic, and desmoplastic HGPs may be detected at other metastatic sites, e.g. brain, lungs, lymph nodes, and skin [8,9,21,22], these observations may take on even greater importance as additional prognostic indicators. Although the pushing HGP is infrequent to rare, there is evidence that this pattern may correlate with an adverse prognosis [8]. Among the seven cases with pushing HGP studied herein, the single case with 80% pushing pattern was associated with a fatal outcome. The pushing HGP thus merits further study with greater numbers of cases.

Other conventional prognostic factors (gender [female], and resection status [R0]) were significant on univariate analysis but lost this effect on multivariate analysis. In contrast, as would be expected, HGP had no predictive value for metastasis-free survival or early OS in patients from the time of diagnosis of primary CM in this study population.

Unlike UM, CM commonly spreads to a number of organs without any particular predilection [4], and resection of CMLM remains infrequent and controversial. However, as in other malignancies (CRC, breast cancer and UM) with comparable histopathological and statistical results, HGPs holds great promise for the selection of patients who may benefit from surgical or other therapeutic intervention *versus* those who will not benefit because they provide new objective prognostic information. Furthermore, increasing evidence indicates that prognostic and biological information conveyed by HGPs is generalisable to all solid tumours studied thus far. Of particular importance is the ultimate goal of correlating radiological images with HGPs in order to develop non-invasive techniques for the assessment and monitoring of liver metastases [23]. The recent application of machine-learning techniques ('radiomics') to the analysis of radiographic images holds promise for more precise non-invasive detection of HGPs [23]. Perhaps of greatest significance is the fact that HGPs provide important new insights into the biology of metastases and opportunities for therapeutic intervention (see below).

With respect to the substantial risk for aggressive neoplastic progression linked to the replacement HGP, it is important to emphasise that, in the replacement pattern, tumour cells occupy (angiotropism/cooption) and spread (pericytic mimicry) in 'vascular niches' [13]. Accumulating evidence suggests that these perivascular niches are preferential sites for cancer stem cells (or cells with stem/embryonic cell properties), resistance to therapy, protection or escape from the immune response, i.e. an immunologically privileged site, and for the progression and dissemination of cancer [4,8,13,24,25].

These findings provide additional support for the concept that pericytic mimicry/replacement/EVMM represents inherently an ‘extravascular’ (abluminal) phenomenon and is independent of intravasation. Concerning the migratory pathway of angiotropic tumour cells *via* pericytic mimicry, several *in vitro* and *in vivo* observations have demonstrated that angiotropic melanoma cells in CM are able to migrate some distance from the primary tumour [13–16]. Additional studies are needed to confirm distant metastasis by this migratory route. Finally, pericytic mimicry and EVMM seem to follow an embryogenesis-derived programme of tumour spread [13,24]. Furthermore, replacement growth in liver metastases has strong analogies with liver organogenesis [26,27] and embryonic competition [13], supporting the concept that embryonic migratory events recur abnormally during the metastatic process [13,24].

In conclusion, we report for the first time the occurrence of replacement and desmoplastic HGPs in CM liver metastases and their important prognostic value in CM, as in UM and other solid cancers. These results contribute to a better understanding of the biology of CMLM and potentially may be utilised in managing patients with these metastases. These results also support the concept of pericytic mimicry/ EVMM in CM.

Acknowledgements

This work was supported by a National Health and Medical Research Council of Australia (NHMRC) Program Grant. RAS is supported by an NHMRC Practitioner Fellowship grants program. Support from colleagues at Melanoma Institute Australia and the Royal Prince Alfred Hospital and The Ainsworth Foundation is also gratefully acknowledged. We sincerely thank Maud Haon who designed the inset diagram for Figure 1B.

Author contributions statement

RB, PV and CL designed the study, developed the methodology, performed experiments, collected data, and analysed data. RB and CL wrote the manuscript, developed the methodology, collected and analysed data. P-JVD, PV, RB and CL performed statistical analyses and analysed data. RS, KB, AL, GC and AN scanned glass slides and managed glass microslides. RS, KB and AL collected data. All the authors reviewed and approved the manuscript.

References

1. Pawlik TM, Zorzi D, Abdalla EK, *et al.* Hepatic resection for metastatic melanoma: distinct patterns of recurrence and prognosis for ocular versus cutaneous disease. *Ann Surg Oncol* 2006; **13**: 712–720.
2. Agarwala SS, Eggermont AM, O’Day S, *et al.* Metastatic melanoma to the liver: a contemporary and comprehensive review of surgical, systemic, and regional therapeutic options. *Cancer* 2014; **120**: 781–789.
3. Tas F, Erturk K. Recurrence behavior in early-stage cutaneous melanoma: pattern, timing, survival, and influencing factors. *Melanoma Res* 2017; **27**: 134–139.
4. Marcoval J, Ferreres JR, Martín C, *et al.* Patterns of visceral metastasis in cutaneous melanoma: a descriptive study. *Actas Dermosifiliogr* 2013; **104**: 593–597.
5. Aubin JM, Rekman J, Vandenbroucke-Menu F, *et al.* Systematic review and meta-analysis of liver resection for metastatic melanoma. *Br J Surg* 2013; **100**: 1138–1147.
6. Barnhill R, Vermeulen P, Daelemans S, *et al.* Replacement and desmoplastic histopathological growth patterns: a pilot study of prediction of outcome in patients with uveal melanoma liver metastases. *J Pathol Clin Res* 2018; **4**: 227–240.
7. Nielsen K, Rolff HC, Eefsen RL, *et al.* The morphological growth patterns of colorectal liver metastases are prognostic for overall survival. *Mod Pathol* 2014; **27**: 1641–1648.
8. van Dam PJ, van der Stok EP, Teuwen LA, *et al.* International consensus guidelines for scoring the histopathological growth patterns of liver metastasis. *Br J Cancer* 2017; **117**: 1427–1441.
9. Terayama N, Terada T, Nakanuma Y. Histologic growth patterns of metastatic carcinomas of the liver. *Jpn J Clin Oncol* 1996; **26**: 24–29.
10. Frentzas S, Simoneau E, Bridgeman VL, *et al.* Vessel co-option mediates resistance to anti-angiogenic therapy in liver metastases. *Nat Med* 2016; **22**: 1294–1302.
11. Galjart B, Nierop PMH, van der Stok EP, *et al.* Angiogenic desmoplastic histopathological growth pattern as a prognostic marker of good outcome in patients with colorectal liver metastases. *Angiogenesis* 2019; **22**: 355–368.
12. Yeh AC, Ramaswamy S. Mechanisms of cancer cell dormancy – another Hallmark of cancer? *Cancer Res* 2015; **75**: 5014–5022.
13. Lugassy C, Kleinman HK, Vermeulen PB, *et al.* Angiotropism, pericytic mimicry and extravascular migratory metastasis: an embryogenesis-derived program of tumor spread. *Angiogenesis* 2020; **23**: 27–41.
14. Bentolila LA, Prakash R, Mihic-Probst D, *et al.* Imaging of Angiotropism/vascular co-option in a murine model of brain melanoma: implications for melanoma progression along extravascular pathways. *Sci Rep* 2016; **6**: 23834.
15. Wilmott J, Haydu L, Bagot M, *et al.* Angiotropism is an independent predictor of microscopic satellites in primary cutaneous melanoma. *Histopathology* 2012; **61**: 889–898.
16. Van Es SL, Colman M, Thompson JF, *et al.* Angiotropism is an independent predictor of local recurrence and in-transit metastasis in primary cutaneous melanoma. *Am J Surg Pathol* 2008; **32**: 1396–1403.
17. Moy AP, Duncan LM, Muzikansky A, *et al.* Angiotropism in primary cutaneous melanoma is associated with disease progression

- and distant metastases: a retrospective study of 179 cases. *J Cutan Pathol* 2019; **46**: 498–507.
18. Bald T, Quast T, Landsberg J, et al. Ultraviolet radiation-induced inflammation promotes angiotropism and metastasis in melanoma. *Nature* 2014; **507**: 109–113.
 19. Barnhill RL, Ye M, Batistella A, et al. The biological and prognostic significance of angiotropism in uveal melanoma. *Lab Invest* 2017; **97**: 746–759.
 20. Pourhoseingholi MA, Baghestani AR, Vahedi M. How to control confounding effects by statistical analysis. *Gastroenterol Hepatol Bed Bench* 2012; **5**: 79–83.
 21. Latacz E, Caspani E, Barnhill R, et al. Pathological features of vessel co-option versus sprouting angiogenesis. *Angiogenesis* 2020; **23**: 43–54.
 22. Kuczynski EA, Vermeulen PB, Pezzella F, et al. Vessel co-option in cancer. *Nat Rev Clin Oncol* 2019; **16**: 469–493.
 23. Cheng J, Wei J, Tong T, et al. Prediction of histopathologic growth patterns of colorectal liver metastases with a noninvasive imaging method. *Ann Surg Oncol* 2019; **26**: 4587–4598.
 24. Lugassy C, Péault B, Wadehra M, et al. Could pericytic mimicry represent another type of melanoma cell plasticity with embryonic properties? *Pigment Cell Melanoma Res* 2013; **26**: 746–754.
 25. Lugassy C, Scolyer R, Long G, et al. PDGFBR expression in anti-BRAF resistant melanoma: are angiotropic melanoma cells a source of BRAF resistance and disease progression? *J Cutan Pathol* 2014; **41**: 159–160.
 26. Matsumoto K, Yoshitomi H, Rossant J, et al. Liver organogenesis promoted by endothelial cells prior to vascular function. *Science* 2001; **294**: 559–563.
 27. Gordillo M, Evans T, Gouon-Evans V. Orchestrating liver development. *Development* 2015; **142**: 2094–2108.